CHEMMEDCHEM

CHEMISTRY ENABLING DRUG DISCOVERY

Accepted Article

Title: Preparation of Titanocene-Gold Compounds Based on Highly Active Gold-NHeterocyclic Carbene Anticancer Agents. Preliminary in vitro Studies in Renal and Prostate Cancer Cell lines.

Authors: Natalia Curado, Nora Giménez, Kirill Miachin, Aliaga-Lavrijsen Mélanie, Mike Anthony Cornejo, Andrzej A Jarzecki, and Maria Contel

To be cited as: *ChemMedChem* 10.1002/cmdc.201800796

Link to VoR: http://dx.doi.org/10.1002/cmdc.201800796

A Journal of

ChemPubSoc Europe

WILEY-VCH

www.chemmedchem.org

FULL PAPER WILEY-VCH

Preparation of Titanocene-Gold Compounds Based on Highly Active Gold(I)-N-Heterocyclic Carbene Anticancer Agents. Preliminary *in vitro* Studies in Renal and Prostate Cancer Cell lines.

Natalia Curado,[a]# Nora Giménez,[a,b]# Kirill Miachin,[a] Mélanie Aliaga-Lavrijsen,[a,c] Mike A. Cornejo,[a] Andrzej A. Jarzecki,[a,d,e] and María Contel*[a,d-f]

[a] Dr. N. Curado https://orcid.org/0000-0003-3878-1191, K. Miachin, M. A. Cornejo
Department of Chemistry
Brooklyn College, The City University of New York
Brooklyn, NY, 11210, USA.
[a,b] N. Giménez
[b]Departamento de Química-Centro de Síntesis Química de La Rioja (CISQ), Universidad de la Rioja, 2606, Logroño (Spain)
[a,c] M. Aliaga-Lavrijsen
[c]Departamento de Química Inorganica, Instituto de Síntesis Química y Catálisis Homogénea (ISQCH), CSIC-Universidad de Zaragoza, 5009, Zararagoza (Spain)
[a,d,e] Prof. A.A. Jarzecki
[a,d-f] Prof. M. Contel, https://orcid.org/0000-0003-9825-4441,
[d]Chemistry, [e]Biochemistry and [f]Biology PhD Programs,
The Graduate Center, The City University of New York
365 Fifth Avenue, New York, NY, 10016, USA.
Email: mariacontel@brooklyn.cuny.edu
Homepage: http://mariacontel.blog.brooklyn.edu/
# These authors contributed equally to the work.

Supporting information for this article is given via a link at the end of the document.

Abstract: Heterometallic titanocene-based compounds containing gold(I)-phosphane fragments have been extremely successful against renal cancer *in vitro* and *in vivo*. The exchange of phosphane by *N*-heterocyclic carbene ligands to improve or modulate their pharmacological profile afforded bimetallic complexes effective in prostate cancer but less effective in renal cancer *in vitro*. We report here on the synthesis of new bimetallic Ti-Au compounds by incorporation of two highly active gold(I)-N-heterocyclic carbene fragments previously reported derived from 4,5-diarylimidazoles. The two new compounds [(η^5-C_5H_5)$_2$TiMe(μ-mba)Au(NHC)] (NHC = 1,3-Dibenzyl-4,5-diphenylimidazol-2-ylidene *NHC-Bn* **2a**; 1,3-Diethyl-4,5-diphenylimidazol-2-ylidene *NHC-Et* **2b**) with the dual linker (-OC(O)-*p*-C_6H_4-S-) containing both a carboxylate and a thiolate group were evaluated *in vitro* against renal, and prostate cancer cell lines. The compounds were more cytotoxic than previously described Ti-Au compounds containing non-optimized gold(I)-N-heterocyclic fragments. We present studies to evaluate their effects on cell death pathways, migration, inhibition of thioredoxin reductase (TrRx) and vascular endothelial growth factor (VEGF) in prostate PC3 cancer cell lines. The results support that the incorporation of a second metallic fragment like titanocene to biologically active gold(I) compounds improves their pharmacological profile.

Introduction

Metal-based drugs have experienced a resurgence as prospective cancer chemotherapeutics with a growing number of compounds active against tumors *in vivo* and some in current clinical trials.[1,2] Current efforts have been focused in the use on non-conventional metallodrugs (those with a mode of action different from that of cisplatin)[3,4] as well as in understanding their mode of action,[5] their effects in the immune system[6] and in developing agents that can be photoactivated[7] or delivery systems[8] that may improve their pharmacological profiles. The potential of heterometallic compounds (compounds with two or more different metals) in cancer therapy has been recently highlighted.[9] The hypothesis (first described by Casini and co-workers)[10] is that the incorporation of two different biologically active metals in the same molecule may improve their antitumor activity as a result of metal specific interactions with distinct biological targets (*cooperative effect*) or by the improved chemicophysical properties of the resulting heterometallic compound (*synergism*).

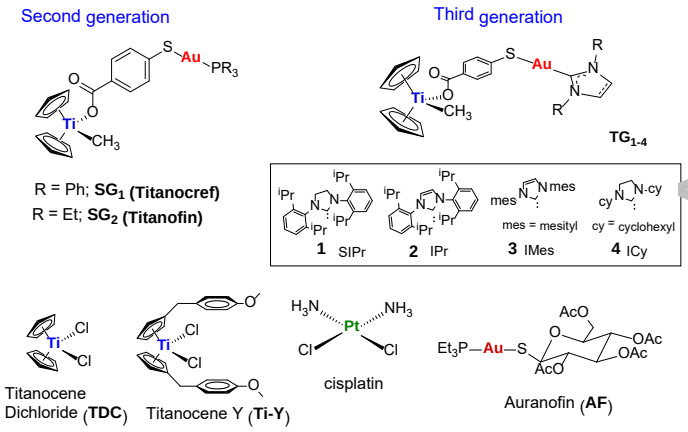

Figure 1. Second and third generation bimetallic compounds based on titanocene and gold(I) fragments with relevant anticancer properties.[5-7] Structure of cisplatin, Auranofin (AF), titanocene dichloride (TDC) and Titanocene-Y (Ti-Y) used as controls in some of the biological experiments or mentioned in the manuscript.

Our group at Brooklyn College has described a variety of compounds based on gold(I) biologically active fragments (either containing phosphanes PR_3 or *N*-heterocyclic carbenes NHC and a second metallic fragment (based on titanocene $[TiCp_2]$[11-16] or arene ruthenium(II) $[Ru(p\text{-cymene})Cl_2(dppm)]$[17-19] derivatives). We unveiled the potential of these compounds as chemotherapeutics against renal, colorectal and prostate cancers (including mechanistic and *in vivo* studies). Second generation titanocene-based compounds (**SG_1** and **SG_2** in figure 1) based on the bifunctional ligand mba = -OC(O)-*p*-C_6H_4-S- (derived from 4-mercaptobenzoic acid H_2mba) resulted extremely efficacious in human clear cell renal carcinoma Caki-1 cells[14,15] and xenograft mice[14] models. We demonstrated that these bimetallic compounds were more potent and affected a broader spectrum of molecular targets and cellular behaviors than any single isolate monometallic derivative.[15]

Third generation titanocene-based compounds (**TG_{1-4}**)[16] containing [Au(NHC)] fragments (instead of $[Au(PR_3)]$) resulted much less cytotoxic (500-100 times less efficient) on the renal cancer cells than the second generation compounds **SG_{1-2}**. They however displayed relevant *in vitro* cytotoxic and apoptotic behavior and antimigratory properties in human prostate cancer (PC3) cell lines.[16]

We report here on the preparation of modified third generation titanocene-gold bimetallic compounds of the type $[(\eta_5\text{-}C_5H_5)_2TiMe(\mu\text{-mba})Au(NHC)]$ (**2a** and **2b** in Scheme 1) based on two highly active gold(I) compounds containing N-heterocyclic carbenes ([AuX(NHC)]; NHC = 1,3-Dibenzyl-4,5-diphenylimidazol-2-ylidene *NHC-Bn*; X = Cl **a**; 1,3-Diethyl-4,5-diphenylimidazol-2-ylidene *NHC-Et; X = Br* **b**) already described.[20,21] Both gold(I)-NHC compounds had been synthesized on the basis of relevant pharmacological properties of 4,5-diarylimidazoles[22] and the well-known antitumor properties displayed by gold(I) compounds containing either phosphanes [23,24] or N-heterocyclic carbenes.[25,26] Compound **a** (described by Tacke and co-workers[20,26,27]) and a variation with the 2',3',4',6'-tetra-O-acetyl-β-D-glucopyranosyl-1'-thiolate showed very good activity against a wide range of human cancer cell lines from the NCI 60 cell line panel, and relevant tumor growth inhibition *in vivo* for a human clear cell renal carcinoma Caki-1 xenograft mice model.[27] More recently compound **a** has been bioconjugated to an engineered antibody (Thiomab LC-V2050) via cysteine conjugation. The anti-proliferative activity of this ADC in HER2 positive breast cancer cell line showed a promising moderate improvement as compared to the gold-complex drug.[28] Compound **b**, described by Gust and co-workers in 2011, was found to be cytotoxic (low or sub-micromolar range) in breast and colon cancer cell lines.[21]

We hypothesized that the incorporation of these highly cytotoxic gold(I) compounds and titanocene in the same molecule would improve their pharmacological profile. In addition to the synthesis, characterization and study of the stability of the new titanocene-gold compounds (and their monometallic precursors containing the mba linker, **1a** and **1b** in Scheme 1), we report on their cytotoxicity in human renal (Caki-1) and prostate (PC3) cancer cell lines, and their selectivity. We also report on the type of cell death induction, anti-migratory properties and inhibitory properties of TrRx and VEGF in prostate PC3 cancer cell lines for bimetallic compound **2a** and precursor **1a**. We include comparisons with the previously described[19] [AuX(NHC)] compound **a**.

Results and Discussion

Synthesis, characterization and stability studies

The new compounds $[(\eta^5\text{-}C_5H_5)_2TiMe(\mu\text{-mba})Au(NHC)]$ (*NHC-Bn* **2a**; *NHC-Et* **2b** in Scheme 1) are synthesized by reaction of precursors [Au(Hmba)(NHC)] (*NHC-Bn* **1a**; *NHC-Et* **1b**) and $[(\eta\text{-}C_5H_5)_2TiMe_2]$ (Equation 1) via a procedure already reported.[14-16] All new compounds were obtained as white (**1a-b**) or yellow (**2a-2b**) solids. The synthesis and characterization details are provided in the experimental section and NMR, IR and ESI-MS-HR spectra are provided in the SI. The structures for the bimetallic compounds in Scheme 1 are proposed on the basis of analytical and spectroscopic data and by comparison with structurally-related compounds.[14-15] Compounds **2a** and **2b** are stable in solid state in air and at 5°C for months. ESI^+-MS-HR spectra shows the parent peak for compound **2b** as well as a peak (S17 and S18) for trimetallic species containing the $Ti(\eta_5\text{-}C_5H_5)_2Me(\mu\text{-mba})$ scaffold and two [Au(*NHC-Et*)] fragments (Figure S17). The identification of mutimetallic species by MS spectrometry (due to coordination of more than one $[AuL]^+$ fragments to sulfur atoms under these conditions) is well known.[29] The ESI^+-MS-HR spectra for **2a** only shows the trimetallic species (S15 and S16).

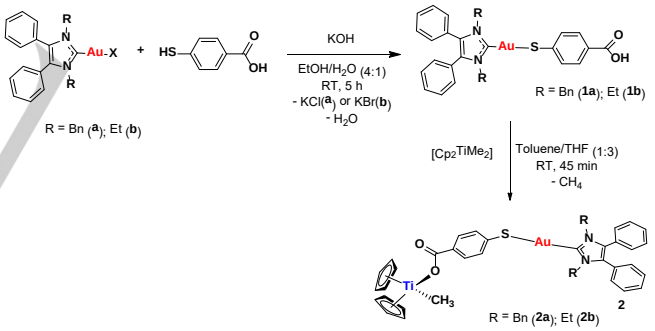

Scheme 1. Preparation of $[(\eta\text{-}C_5H_5)_2TiMe(\mu\text{-mba})Au(NCH)]$ (*NHC-Bn* **2a**; *NHC-Et* **2b**).

The diagnostic technique to assess the type of coordination of the carboxylate group from the mba ligand is IR spectroscopy. On the basis of the difference between symmetric and antisymmetric stretching bands in the solid state IR spectra of compounds **2a** and **2b** it is safe to propose a monodentate bonding for the carboxylate[30,31] as previously described by our group for both phosphine and NHC ligands, which was corroborated by DFT calculations.[14-16] In addition, we have performed more detailed DFT calculations in order to identify the coordination mode of the carboxylic group in bimetallic complexes **2a** and **2b** (see Figure 2 and in the SI, Table S1 and Figures S29 and S30). The relative position of symmetric and asymmetric stretching bands of the carboxylate groups can

distinctly characterize monodentate versus bidentate complexes. Both bands are observed in the experimental IR spectra; the symmetric strong band at 1284 cm^{-1} and the asymmetric moderate band at 1635 cm^{-1} for both **2a** and **2b** complexes. The observed difference of about 350 cm^{-1} indicates the monodentate coordination for these complexes. Moreover, the monodentate coordination mode was confirmed by DFT calculations where both coordination modes were modeled and compared to experimental spectra (Figures S29 and S30). For monodentate complexes the intense symmetric stretching band was computed around 1288 cm^{-1}, and the asymmetric bands at 1690 cm^{-1} that agrees with experimental bands and confirms the coordination mode. In contrast, for bidentate complexes the intense symmetric stretching band computed at 1456 cm^{-1} and the asymmetric band around 1523 cm^{-1} it is not in accordance with experimental spectra and excludes the bidentate coordination mode for these complexes. The most relevant distances calculated are collected in table S1 (SI).
Unfortunately, we could not obtain crystals of enough quality for bimetallic compounds **2a** and **2b** for X-ray diffraction studies.

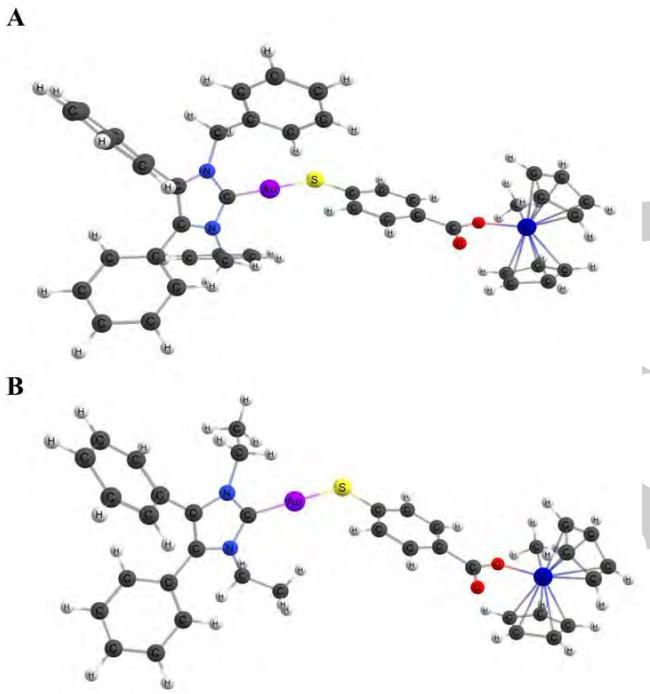

Figure 2. Structure and atom labeling of compounds **2a** (A) and **2b** (B), shown at the energy-minimized geometry. For distances and angles see Table S1 in SI.

The crystal structures of the monometallic precursors **1a** and **1b** were determined by X-ray (Figure 3 and in SI, Figures S31-S33 and Tables S2 and S3). These structures are relevant due to the biological activity found for these precursors (see biological activity section). We have previously reported on the crystallography of compounds containing the mba linker and phosphane or N-heterocyclic carbene ligands.[14-16] The structure of **1a** is depicted in Figure 3A. Its monomeric structure is almost identical to that obtained with a different NHC (ligand **3** in Figure 1) and reported by us recently.[16] The structure of **1b** is included in the SI information (S32) as it is extremely similar as well. For **1a** the environment of the gold atoms is close to linear [C-Au-S 177.93(5)°] (Figure 3). A crystal structure of an analogue of compound **a** ((1,3-Di(*p*-methoxybenzyl)4,5-di(*p*-isopropyl phenyl)imidazol-2-ylidene)gold(I) chloride) had been already reported by Tacke *et al*.[20] The distance Au-C(1) of 2.0129(19) Å for **1a** is close to that of compound **a** analogue of 1.988(3) Å. The angle of C(1)-Au-Cl(1) for the Tacke analogue is 180° (linear as in the case of **1a**). For **1b** (Figure S32 in SI) the angle is 174.33(8)° (still close to linearity) and the distortion most plausibly due to the supramolecular arrangement (Figure S33). A crystal structure of an analogue of **b** ([1,3-Diethyl-4,5-bis(4-fluorophenyl)imidazol-2ylidene]gold(I) bromide) was also reported by Gust *et al*.[21] In this case the distance Au(1)−C(1) was 1.988(9)Å and the angle C(1)−Au(1)−Br(1) 178.3(2)°, again within the same range as for **1b** where the C(1)-Au(1) distance is 2.010(3) Å and the angle a little shorter (174.33(8)°).

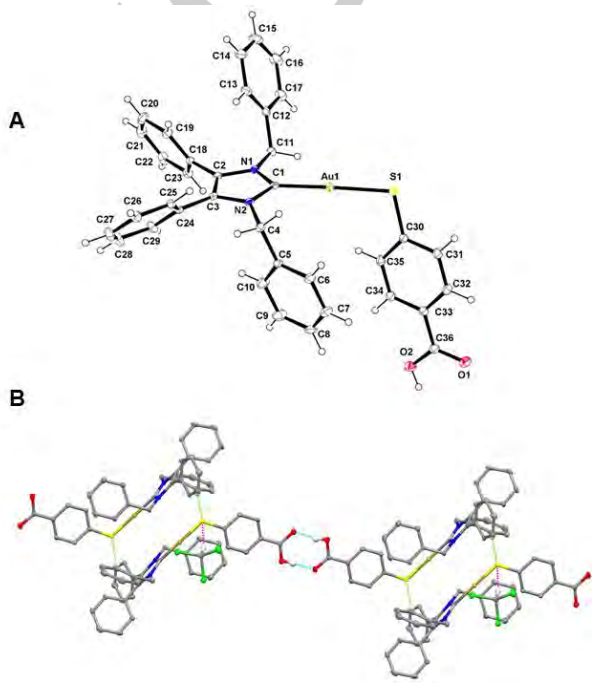

Figure 3. A. ORTEP view of the molecular structure of **1a** showing the labelling scheme. The labels for hydrogen and some carbon atoms are omitted for clarity. B. Crystal packing of **1a***$CHCl_3$ showing the intermolecular contacts. The supramolecular packing is formed by hydrogen bonds (light blue lines) (1.782 Å), S···H_{CHCl3} (2.534 Å) and S···H_{Ph} (2.874 Å) (green lines) interactions.

The most relevant characteristic of these compounds in solid state, is their ability to form supramolecular species via hydrogen bonding and in some specific cases via gold-gold interactions. In the case of compound **1a** (Figures 3 and S31) the monomers organize into chains that are linked by short O-H bonds (1.782 Å). There are additional interactions between monomers and $CHCl_3$ solvent molecules (interactions between the sulfur atom and one H from the $CHCl_3$ molecule of 2.534 Å) as well as weaker interactions between the sulfur atom in one monomer and one hydrogen from a phenyl group in another monomer (2.874 Å). In the case of compound **1b** (Figure S33) there are also short O-H bonds (1.871 Å) linking two different monomeric units and longer interactions between an oxygen from a monomer and one hydrogen from a phenyl group from a different monomer (2.589 Å).In these structures there are no appreciable gold-gold interactions. The shorter Au-Au distance observed for Au···Au 3.659 Å (1a) is a little above the sum of the

van der Waals radii of ca. 3.6 Å. The only compound that displayed monomers linked by gold-gold bonds, [(η^5-$C_5H_5)_2$TiMe(μ-mba)Au(PEt_3)] (**SG2** in figure 1) has been reported recently.[16]

The stability of compounds **2a** and **2b** was evaluated by ^{1}H NMR spectroscopy in DMSO and DMSO/PBS (5:1) and by mass spectrometry over time (see SI). NMR experiments were performed in DMSO-d^6 and in mixtures of DMSO-d^6/PBS-D_2O. The stability study of compounds **2a** and **2b** by ^{1}H NMR in DMSO-d^6 showed half-life values of 18 and 6 hours, respectively, considerably longer than former derivatives containing other NHC (third generation **TG_{1-4}** derivatives in Figure 1) with half-lives ranging from 1 to 3 hours. The half-lives of **2a** and **2b** are also longer or in the same range as second generation compounds **SG_{1-2}** (Figure 1). Mass spectrometry further supports the presence of species containing both titanium and gold in 1% DMSO/PBS solution after 24 hours (see SI). We have shown in the past that the cyclopentadienyl ligands are dissociated over time, something we also observe for **2a** and **2b**.[14-16] In general, for titanocene-gold compounds we have been able to prove the co-localization of both metals (titanium and gold) both in cancer cells[14-16] and in tumors.[32] This fact indicates that the bimetallic compounds are pro-drugs that decompose into biological active species still containing a Ti-Au core.[32]

Biological activity

Cytotoxicity, selectivity and cell death

The cytotoxicity of the bimetallic compounds [(η^5-$C_5H_5)_2$TiMe(μ-mba)Au(NHC)] (NHC = *NHC-Bn* **2a**, *NHC-Et* **2b**), monometallic gold precursors [Au(Hmba)(NCH)] (NHC = *NHC-Bn* **1a**, *NHC-Et* **1b**), the gold cytotoxic compounds ([AuX(NHC)]; NHC = *NHC-Bn*; X = Cl **a** "Tacke"; *NHC-Et; X = Br* **b** "Gust") already described,[11,12] and monometallic titanocene Y was evaluated. Titanocene Y (a compound described by the group of Tacke[33]) is considered a good benchmark for titanocenes due to its high activity in breast,[34,35] and renal[36] cancer *in vitro* and *in vivo*. For comparative purposes, the cytotoxic profile of cisplatin and Auranofin was also determined. In this assay, human clear-cell renal carcinoma Caki-1, human prostate PC3 cells and non-tumorigenic human fetal lung fibroblasts (IRM-90) were incubated with the above described compounds for 72 hours. The compounds were assayed by monitoring their ability to inhibit cell growth using the PrestoBlue™ Cell Viability assay (see Experimental Section). The results are summarized in Table 1.

The heterometallic compounds **2a** and **2b** are considerably more toxic to the renal (Caki-1) and prostate cancer cell lines (PC3) than cisplatin and Titanocene Y. They have a cytotoxicity similar to that of Auranofin but their selectivity is better. In this case and while gold compound [AuCl(*NHC-Bn*)] **a** had shown a cytotoxicity in the low micromolar range for these cell lines,[21] we found that the IC_{50} value with our method (PrestoBlue™ Cell Viability assay, 72 hours**)** was 27.7 ± 0.5 μM (similar to that of cisplatin and Titanocene Y). For gold compound **b** the cytotoxicity in these renal and prostate cancer cell lines had not been reported. The cytotoxicity of the compound with the mba linker **1a** improves considerably with respect to compound **a** and the cytotoxicity of the bimetallic **2a** is similar of that of **1a** but its selectivity improves. For **b** the results are different since this compound resulted highly cytotoxic for both the renal and prostate cell lines while having a very good selectivity (see Table 2). The modification of incorporating the mba linker (compound **1b**) decreases the cytotoxicity and selectivity which then improves by incorporation of the titanocene fragment (compound **2b**) but still this compound does not result as good as **b** in terms of cytotoxicity and selectivity combined. It is important to note that the cytotoxicity of the bimetallic compounds **2a** and **2b** in the renal cancer cell line Caki-1 improves considerably (5-13-fold) when compared to previously described third generation compounds [(η_5-$C_5H_5)_2$TiMe(μ-mba)Au(NHC)] (**TG_{1-4}** in Figure 1) which displayed IC_{50} values in the range of 21-51 μM for this cell lines. For the prostate cancer cell lines the IC_{50} value of **2b** (9.5 μM) is in the range for those described for **TG_{1-4}** (9.8-17 μM) and compound **2a** has a lower value at 3.9 μM. We choose compounds **a**, **1a** and **2a** and the cell line PC3 for further studies for better comparison with third generation compounds **TG_{1-4}** (in Figure 1). We also chose Auranofin as a control for our experiments (as we have done previously with other titanocene-gold compounds[14-16]).

Table 1. IC_{50} values (μM) for Caki-1, PC3 and IMR-90 treated with bimetallic **2a**, **2b** and monometallic **a**, **1a**, **b**, **1b**. Monometallic compounds Auranofin (**AF**), titanocene-Y (**Ti-Y**) and cisplatin (Structures in Chart 1) were used as controls.[a]

Compound	Caki-1	PC3	IMR-90
a	27.7 ± 0.5	24.8 ± 0.5	84.4 ± 6.2
1a	3.8 ± 0.1	3.7 ± 0.1	7.8 ± 0.5
Ti-Au 2a	4.3 ± 0.1	3.9 ± 0.1	15.1 ± 3.3
b	2.01 ± 0.3	11.8 ± 1.4	89.0 ± 7.7
1b	9.2 ± 0.4	22.2 ± 0.4	38.1 ± 2.6
Ti-Au 2b	5.0 ± 0.01	9.5 ± 0.3	12.6 ± 0.1
Auranofin	2.8 ± 0.6[b]	3.6 ± 0.005	3.7 ± 0.4[b]
Titanocene-Y	29.4 ± 4.2	58.1 ± 11.2	>100
Cisplatin	23.9 ± 2.4[b]	6.7 ± 2.8	3.9 ± 0.5[b]

[a] Compounds **a**, **1a**, **1b** and **2a** were dissolved in a 1:1 solution of Triethylglycol and DMSO (1%), while compounds **b**, **2b**, **AF** and **Ti-Y** were dissolved in 1% DMSO. Cisplatin was dissolved in H_2O. All compounds were further diluted in cell culture media before addition to cells for a 72 h incubation period. The IC_{50} values are reported with the standard deviation of the sample mean (triplicates). [b] Values previously reported in reference [10].

Following the evaluation of the cytotoxicity of the compounds we proceeded to evaluate how the cells died. For this assay PC-3 cells were incubated with monometallic gold compounds **a**, **1a** Auranofin and bimetallic **2a** at the IC_{50} concentration for 72 hours. We observed that all the compounds induce apoptosis at their IC_{50} concentration (Figure 4). From these data, it can be deduced that compounds **a**, **1a** and **2a** induce similar apoptosis in prostate PC3 cancer cell lines after 72 hours (45-50%) while **AF** is more apoptotic (73%) in the same cell population. It should be highlighted however, that monometallic compound **a** has a considerably higher IC_{50} value than bimetallic **2a** and thus, the

incorporation of the titanoce metallic fragment improves the apoptotic properties.

Second generation compounds (**SG$_{1-2}$**) had also diplayed relevant apoptotic behavior in renal cancer cells.[5-6] Third generation compounds [(η^5-C_5H_5)$_2$TiMe(μ-mba)Au(NHC)] (**TG$_{1[4}$** in Figure 1) displayed apoptosis in PC3 cell lines as the major mode of cell death. However a quantification of apoptotic cells versus viable cells was not performed.[16] We have hypothesized that the apoptotic behavior of bimetallic titanocene-gold species comes from the two different metallic fragments[9,32] since both gold[38,39] and titanocene dichloride[40] are known to induce apoptosis in several cancer cell lines.

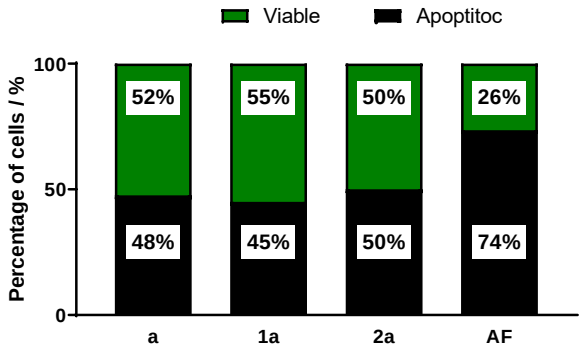

Figure 4. Cell death induced in PC3 cells by the IC_{50} of **a**, **1a, 2a** and Auranofin measured by flow cytometry after 72 h of incubation. The bar graph represents the quantification of cell death. Compound **a**, **1a** and **2a** induced apoptosis in 47%, 45 and 50% of the cell population while **AF** induced apoptosis in 73% of the cell population.

Inhibition of migration by selected compounds

Relevant anti-migration[14-16] and anti-invasion[15] properties have been found for titanocene-gold compounds in renal cancer cell lines, especially for the second generation compounds **SG$_{1-2}$**. This is very important for the development of new anticancer chemotherapeutics as increased local cell migration and distal invasion are hallmarks of metastasis.[41] Two third-generation bimetallic titanocene-gold compounds **TG$_1$** and **TG$_2$** (in Figure 1) provided a reduction of migration of 46% and 55% in prostate cancer PC3 cells. The effect of compounds **a**, **1a**, **AF** and bimetallic **2a** on migration (at IC_{20} concentration) was determined using a wound-healing 2D scratch assay on a collagen-coated plate (Figure 5A). IC_{20} amounts are chosen because for these type of compounds at those concentrations around 80% of cells are alive and the effect measured is not due to cell death.[15]

Figure 5B shows that bimetallic compound **2a** reduces migration in ca. 92%. This reduction is significantly higher than that of Titanocene-Y (19%)[16] and that of the third generation bimetallic compounds already described **TG1** and **TG2** (Figure 1).[7] It is also slightly higher that that of AF (85%) in this cell line. For the renal cancer cell line Caki-1 we found that AF had a sightly or moderately higher migration inhibition than bimetallic compounds SG1-2.[15] We also found that the migration produced by bimetallic **2a** is higher than that of monometallic precursor **1a** or previously described compound [AuCl(NHC)] **a** (92% **2a** versus 66% **1a** and 71% **a** at their corresponding IC20 values) indicating again that there is an advantage in linking the titanocene fragment to the monometallic gold compound **a**.

These results are quite significant since we have been able to correlate anti-migration with anti-invasion properties for titanocene-gold derivatives.[15] This means that these compounds may indeed have the potential to act as promising antimetastatic agents. Singaling molecules linked to migration and metastasis have also been inhibited significantly by second generation Ti-Au in renal cancer Caki-1 cell lines.[15] The potential for chemotherapeutics displaying both cytotoxicity and antimetastatic properties should be underscored.

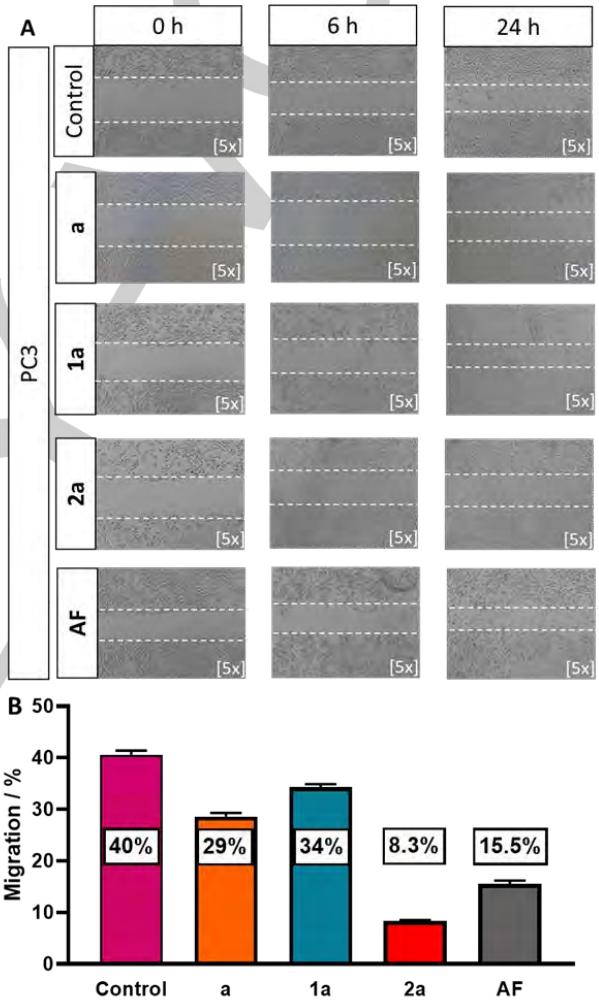

Figure 5. Cell migration assay for bimetallic compound **2a**, and monometallic compound **a**, **1a** and **AF**. Inhibition of migration (2D wound-healing scratch assay) by the IC_{20} of each compound. The assay indicates that **2a**, **1a**, and **AF** interfere with PC3 migration. A. The panels show the width of the scratch at 0, 6, and 24 after it was inflicted. B. The bar graph represents the quantification of the cell migration at 48h relative to the 0h time-point.

Inhibition of Thioredoxin Reductase (TrxR) and Vascular Endothelial Growth Factor (VEGF) by selected compounds

Modification in the anti-oxidant profile of cancerous cells is characteristic of chemoresistance and is often accompanied by the overexpression of thioredoxin reductase (TrxR).[42,43] Increases in TrxR levels are critical to the mechanism of

cisplatin-resistant cells which renders it an attractive drug target.[44-46] Additionally, preventing the supply of nutrients and oxygen to the tumor site will hinder the tumor progession. Vascular endothelial growth factor (VEGF) is a key growth factor in angiogenesis, which potently stimulates the formation of blood vessels which allows tumor growth and progression.[47,48,49] Gold compounds, including, Auranofin have been reported to significantly inhibit TrxR levels[14-16] and VEGF levels[15] in clear cell renal carcinoma Caki-1 and prostate cancer PC3 cell lines.

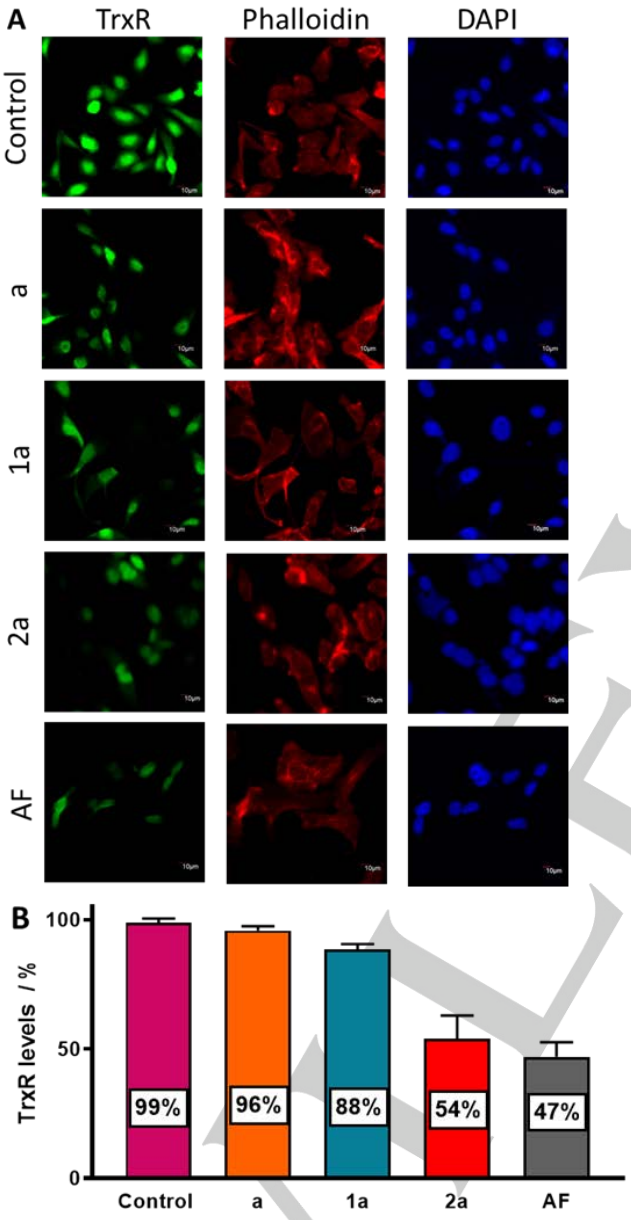

Figure 6. A. Immunofluorescent analysis of TrRx level upon treatment with control (0.1 % DMSO), **a**, **1a**, **2a** or Auranofin (**AF**) in 0.1% DMSO for 24 h. Thioredoxin reductase (green) in the PC3 cells and its levels are changed in response to treatment with compounds of interest. B. Quantitative analysis of TrRx levels using ImageJ showing significant decreasing the enzyme level following exposure to **2a** and **AF** compared to control. All data in bar graphs represent mean ± SD of two independent experiments ($p < 0.05$).

Immunocytochemistry is a technique that allows direct visualization of the presence, intensity or absence of a cellular protein of interest through the use of fluorescently labeled antibodies. The fluorescent signal emitted results from the highly specific binding of antibodies to their unique antigens.[50,51] In order to detect all cells, the DNA-labeling dye DAPI is used as it labels in blue each nuclei corresponding each to one cell. DAPI positive spots are used to obtain the total cell count in a given sample. Phalloidin is used to label the actin protein, which makes up most of mammalian cell's cytoskeleton and here emits a red signal. Through phalloidin positive staining cytoskeletal integrity can be assessed. In the experiment described here, we have also used a fluorescent-labeled antibody for TrxR, colored green, and for VEGF, colored yellow. Through this experiment we aim to determine to which extent the treatment with the metallo-complexes being studied inhibit or lead to the overexpression of TrRx and VEGF.

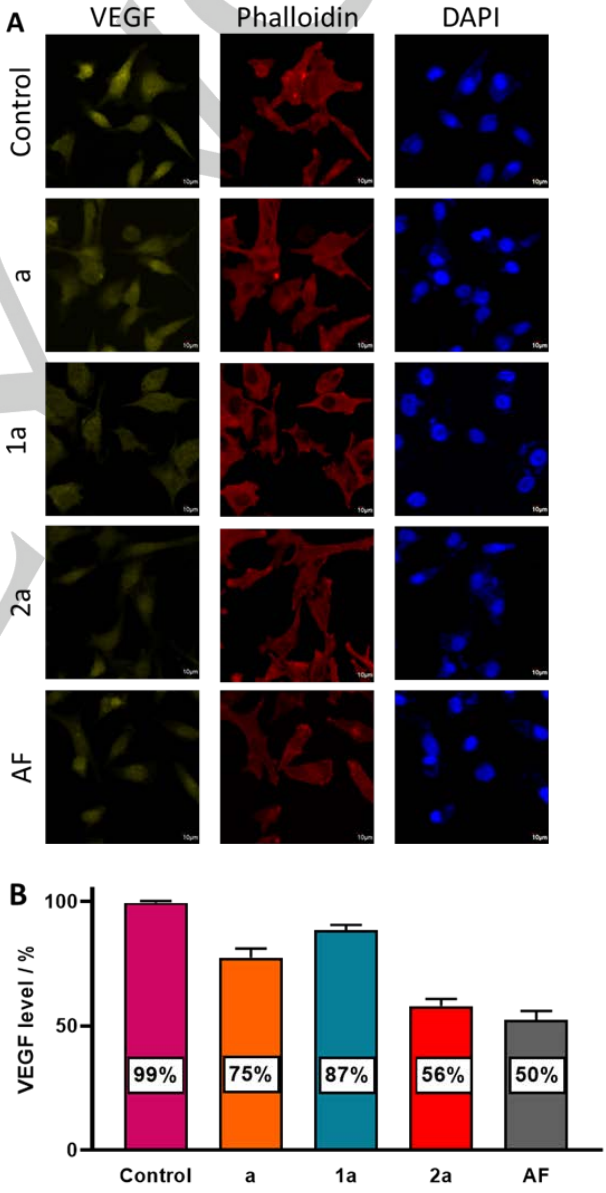

Figure 7. A. Immunofluorescent analysis of VEGF level upon treatment with control (0.1 % DMSO), **a**, **1a**, **2a** or Auranofin (**AF**) in 0.1% DMSO for 24 h. VEGF (yellow) in the PC3 cells and its levels are changed in response to treatment with compounds of interest. B. Quantitative analysis of VEGF levels using ImageJ showing significant decreasing the protein levels following exposure to **2a** and **AF** compared to control. All data in bar graphs represent mean ± SD of two independent experiments ($p < 0.05$).

The results obtained for the inhibition of TrRx experiment (Figure 6) indicate that **a** ([AuCl(*NHC-Bn*)] or "Tacke" compound) inhibits only 3% of TrxR in the assay conditions (IC_{20} concentrations and 24 h incubation time). Compound **1a** inhibits 12% of TrxR activity while **2a** inhibits TrxR activity by 38% a reflected by the decrease of TrxR positive cells. The inhibition of TrxR by the bimetallic compound **2a** is within the same range than that of **AF** that with this assay affords an ihibition of 46%. The results obtained for the inhibition of VEGF experiment (Figure 7) indicate that **a** ([AuCl(*NHC-Bn*)] or "Tacke" compound) reduces 25% of VEGF expression in assay conditions (IC_{20} concentrations and 24 h incubation time). Compound **1a** reduces 13% of VEGF activity while **2a** reduces 44% of VEGF activity. Their reduction is reflected by the decrease of VEGF in positive cells (**control**). The reduction of VEGF by the bimetallic compound **2a** is also within the same range that of **AF** (50% of VEGF reduction).

It is clear that the incorporation of the titanocene fragments to compound **a** improves significantly its TrxR and VEGF inhibitory properties as we have already reported for second[14,15] and third generation[16] titanocene-gold compounds containing phosphane and N-heterocyclic carbene ligands. The improvement presented here is however quite remarkable.

Conclusions

In conclusion, we have synthesized bimetallic compounds containing titanocenes and gold(I)-N-heterocyclic carbene fragments which were already known to display relevant anticancer properties *in vitro* and *in vivo*. We have demonstrated that the incorporation of the titanocene fragment improves or does not decrease the cytotoxicity in the human cancer cell lines Caki-1 and PC3. We have demonstrated that a selected bimetallic compound derived from monometallic "Tacke" [AuCl(*NHC-Bn*)] has an improved pharmacological profile in terms of apoptosis, inhibition of migration, and inhibition of thioredoxin reductase and VEGF in prostate cancer cell lines with respect to the monometallic bioactive gold compound. The work presented here supports the idea that bimetallic compounds can indeed be designed to contain two different active metal-based fragments (and allow for synergistic and/or cooperative effects) by judicious choice of the linker.

Experimental Section

General information and instrumentation for synthesis, characterization and stability studies of the new compounds

NMR spectra were recorded in a Bruker AV400 (^{1}H-NMR at 400 MHz and $^{13}C\{^1H\}$ NMR at 100.6 MHz). Chemical shifts (δ) are given in ppm and coupling constants (*J*) in Hertz (Hz), using $CDCl_3$, d^6-DMSO or PBS-D_2O as solvent, unless otherwise stated. ^{1}H and ^{13}C NMR resonances were measured relative to solvent peaks considering tetramethylsilane = 0 ppm. IR spectra (4000-500 cm^{-1}) were recorded on a Nicolet 6700 Fourier transform infrared spectrophotometer on solid state (ATR accessory). Elemental analyses were performed on a Perkin-Elmer 2400 CHNS/O series II analyzer by Atlantic Microlab Inc. (US). Mass spectra electrospray ionization high resolution (MS-ESI-HR) were performed on a Waters Q-Tof Ultima. The theoretical isotopic distributions have been calculated using enviPat Web 2.0.

Synthesis and characterization

[AuCl(tht)],[52] [AuX(NHC)] (X = Cl, Br),[20,21] and Cp_2TiMe_2[53] were prepared as previously reported. Chemicals were purchased as indicated: Cp_2TiCl_2, $H[AuCl_4]$ (STREM Chemicals), 4-mercaptobenzoic acid (H_2mba) and Methyl Lithium solution (1.6M) (Sigma Aldrich). Reaction solvents were purchased anhydrous from Fisher Scientific (BDH, ACS Grade) and Sigma-Aldrich, used without further purification, and dried in a SPS machine and kept over molecular sieves (3 Å, beads, 4-8 mesh), otherwise over sodium if necessary. Deuterated solvents were purchased from Cambridge Isotope Laboratories, Inc. and were kept over molecular sieves (3 Å, beads, 4-8 mesh). Celite (Celite 545, Diatomaceous Earth) was purchased from VWR International and used as received.

General Procedure for [Au(Hmba)(NHC)] (**1a, 1b**). H_2mba (0.061 g, 0.395 mmol) was added to a solution of KOH (0.022 g, 0.395 mmol) in 20 mL of ethanol (16 mL) and water (4 mL) and stirred for 20 minutes at room temperature. [AuX(NHC)] (X = Cl, Br) (0.250g, 0.395 mmol) was added to the previous solution and stirred for 5 hours. Solvents were removed under reduced pressure, and the residue was washed with water (3 × 5 mL) and 10 ml of mixture of diethyl ether /hexane (3:2) to afford **1a, 1b** as white solids. **1a** (*NHC-Bn*): 81% yield (0.241 g). Anal. Calcd. for $C_{34}H_{43}AuN_2O_2S$: C, 57.60; H, 3.86; N, 3.73; S, 4.27. Found: C, 57.40; H, 3.77; N, 3.66; S, 4.15. ^{1}H NMR ($CDCl_3$): δ 5.49 (s, 4H, CH_2), 7.04 (d, $^3J_{HH}$ = 7.2 Hz, 4H, ArH), 7.10 (dd, $^3J_{HH}$ = 6.7 Hz, $^2J_{HH}$ = 2.5 Hz, 4H, ArH), 7.24-7.29 (m, 10H, ArH), 7.34 (t, $^3J_{HH}$ = 7.3 Hz, 2H, ArH), 7.52 (d, $^3J_{HH}$ = 8.4 Hz, 2H, ArH), 7.68 (d, $^3J_{HH}$ = 8.5 Hz, 2H, ArH). $^{13}C\{^1H\}$ NMR ($CDCl_3$): δ 52.64 (s, CH_2), 123.12 (s, 4-C_6H_4), 127.24 (s, 2-C_6H_5), 127.33 (s, 1-C_6H_5), 128.12 (s, 3-C_6H_5), 128.63 (s, 3-C_6H_5), 128.71 (s, 4-C_6H_5), 129.37 (s, 4-C_6H_5), 129.44 (s, 3-C_6H_4), 130.68 (s, 2-C_6H_5), 131.87 (s, 2-C_6H_4), 132.10 (s, C-imidazole), 135.91 (s, 1-C_6H_5), 153.81 (s, 1-C_6H_4) 172.07 (s, C=O), 182.40 (s, C-carbene). IR (cm^{-1}): 2947 m,br (OH), 2322 m, 1667 s, 1580 s (v_{asym} CO_2), 1417 m, 1281 s (v_{sym} CO_2), 1168 s, 1084 s, 766 s. MS (ESI): m/z Calcd 750.67. Found: 997.35 $[NHC\text{-}Au\text{-}NHC]^+$. **1b** (*NHC-Et*): 77% (0.174 g). Anal. Calcd. for $C_{26}H_{25}AuN_2O_2S$: C 49.84; H 4.02; N 4.47; S 5.12. Found: C, 49.56; H, 4.02; N, 4.66; S, 4.89. ^{1}H NMR (CD_3Cl_3): δ 1.35 (t, $^3J_{HH}$ = 7.21 Hz, 6H, CH_3), 4.24 (q, $^3J_{HH}$ = 7.27 Hz, 4H, CH_2), 7.20-7.22 (m, , $^2J_{HH}$ = 1.85Hz, 10H, ArH), 7.36-7.37 (m, , $^2J_{HH}$ = 1.85 Hz, $^3J_{HH}$ = 5.17 Hz, 2H, ArH), 7.73 (d, $^3J_{HH}$ = 8.54 Hz, 6H, ArH), 7.79 (d, $^3J_{HH}$ = 8.54 Hz, 4H, ArH). $^{13}C\{^1H\}$ NMR (CD_3Cl_3): δ 17.23 (s, CH_3), 44.33 (s, CH_2), 127.93 (s, 4-C_6H_4), 129.01 (s, 2,4-C_6H_5), 129.47 (s, 1-C_6H_4), 129.67 (s, 2-C_6H_4), 130.63 (s, 2-C_6H_5), 131.29 (s, C imidazole), 132.10 (s, 3-C_6H_4), 170.88 (s, C = O), 179.76 (s, C-carbene). IR (cm^{-1}): 2953 m,br (OH), 2364 m, 1678 s, 1577 s (v_{asym} CO_2), 1399 s (v_{sym} CO_2), 1259 m, 1116 m, 1080 m, 764 m. MS (ESI): m/z Calcd 626.52. Found: 749.28 $[NHC\text{-}Au\text{-}NHC]^+$.

General Procedure for [(η^5-C_5H_5)$_2$TiMe(μ-mba)Au(NHC)] (**2a,2b**). The corresponding monometallic gold precursor (**1a**, **1b**) (0.220 mmol) was dissolved in tetrahydrofuran (15 mL) and added *via* addition funnel over a solution of Cp_2TiMe_2 (0.046 g, 0.220 mmol) in toluene (5 mL) under nitrogen. The resulting bright orange solution was stirred for 45 minutes at room temperature. The solution was filtered off and the solvents were then removed under reduced pressure to afford an oily solid that was washed with diethyl ether (3 × 5 mL) and hexane (3 x 5 mL) to yield a yellow solid. **2a:** (*NHC-Bn*): 46% yield (0.120 g). Anal. Calcd. for $C_{47}H_{41}AuN_2O_2STi\bullet 1.5H_2O$: C, 58.21; H, 4.58; N, 2.98; S, 3.31. Found: C, 58.05; H, 4.50; N, 2.76; S, 3.55. ^{1}H NMR ($CDCl_3$): δ 0.97 (s, 3H, Ti-CH_3),

5.46 (s, 4H, CH_2), 6.19 (s, 10H, Cp), 7.01 (d, $^3J_{HH}$ = 7.2 Hz, 6H, ArH), 7.06 (d, $^3J_{HH}$ = 6.7 Hz, ArH, 5H), 7.22-7.23 (m, ArH, 5H), 7.27-7.33 (m, ArH, 6H), 7.42 (d, $^3J_{HH}$ = 8.4 Hz, ArH, 2H). $^{13}C\{^1H\}$ NMR ($CDCl_3$): δ 43.98 (s, Ti-CH_3), 52.64 (s, CH_2), 114.26 (s, Cp), 127.31 (s, 2-C_6H_5), 127.37 (s, 1-C_6H_5), 128.04 (s, 4-C_6H_4), 128.58 (s, 3-C_6H_5), 128.64 (s, 4-C_6H_5), 129.24 (s, 4-C_6H_5), 129.29, (s, 3-C_6H_4), 130.69 (s, 2-C_6H_5), 131.68 (s, 2-C_6H_4), 132.02 (s, C-imidazole), 135.91 (s, 1-C_6H_5), 149.69 (s, 1-C_6H_4), 171.77 (s, C=O), 182 (s, C-carbene). IR (cm^{-1}): 2953 m (Cp), 1632, 1580 m (v_{asym} CO_2), 1444 s, 1281 vs (v_{sym} CO_2), 1165 m (Cp), 1083 m (Cp). **2b:** (*NHC-Et*): 26% yield (0.046 g). Anal. Calcd. for $C_{37}H_{37}AuN_2O_2STi•1/2C_7H_9$: 54.29; H, 4.56; N, 3.42; S, 3.92. Found: C, 55.64; H, 5.07; N, 3.21; S, 3.38. ^1H NMR ($CDCl_3$): δ 0.97 (s, 3H, Ti-CH_3), 1.35 (t, $^3J_{HH}$ = 7 Hz, 6H, CH_3), 4.23 (q, $^3J_{HH}$ = 7.4 Hz, 4H, CH_2), 6.20 (s, 10H, Cp), 6.16-7.22 (m, 5H, ArH), 7.35-7.37 (m, 4H, ArH), 7.40 (d, $^3J_{HH}$ = 8.6 Hz, ArH, 2H), 7.63 (d, $^3J_{HH}$ = 8.3 Hz, 2H, ArH). $^{13}C\{^1H\}$ NMR ($CDCl_3$): δ 17.05 (s, CH_3), 43.92 (s, Ti-CH_3), 44.15 (s, CH_2), 114.27 (s, Cp), 127.81 (s, 4-C_6H_4), 128.19 (s, 1-C_6H_5), 128.81 (s, C_6H_5), 129.23 (s, C_6H_5), 129.30 (s, 3-C_6H_4), 130.48 (s, C_6H_5), 131.06 (s, C-imidazole), 131.73 (s, 2-C_6H_4), 150.05 (s, 1-C_6H_4), 171.91 (s, C=O), 182.26 (s, C-carbene). IR (cm-1): 2951 m (Cp), 2338 m, 1635 m, 1581 (v_{asym} CO_2), 1441 m, 1279 m (v_{sym} CO_2), 1168 s (Cp), 1080 s (Cp).

DFT calculations

Calculations of compounds **2a** and **2b** have been carried out with the hybrid density functional method B3LYP as implemented in Gaussian09.[54] Structures were optimized as in a gas phase using 6-311G(d) basis set for all atoms but Au for which the all-electrons DPZ plus polarization basis set was implemented and obtained from the EMSL Basis Set Library.[55,56] The stability of optimized structures has been verified by performing frequency calculations at the same level of theory. Both mono-dentate **2a** and **2b** complexes were computed to be stabilized over the corresponding bi-dentate complexes by about 3.9 kcal/mol. All computed frequencies for optimized structures were positive and their computed normal mode displacements were employed to predict infra-red intensities. Computed spectra were simulated by a Lorentzian broadening with a band width of 30 cm^{-1} on half height of each band.

Crystal structure determination

Colorless single crystals were obtained by slow diffusion of n-hexane into solutions of the complex in $CHCl_3$ (**1a** -30ºC) or THF (**1b** 0 ºC). The diffraction data were collected using graphite monochromatic Mo-Kα radiation with a Bruker APEX-II diffractometer at a temperature of 120 K using the APEX-II software. Structures were solved by Intrinsic Phasing using SHELXT[57] and refined by full-matrix least squares on F^2 with SHELXL.[58] The absorption correction was performed using MULTISCAN[59] with the WINGX program suite.[60] All non-hydrogen atoms were assigned anisotropic displacement parameters. The hydrogen atoms were positioned geometrically, with isotropic parameters 1.2 times the Uiso value of their attached carbon for the aromatic and methylene hydrogens and 1.5 times for the methyl groups. For **1a** one molecule of $CHCl_3$ was found in the asymmetric unit, giving rise the stoichiometry **1a**•$CHCl_3$. The structure of **1b** shows some residual peaks greater than 1 e Å−3 in the vicinity of the gold atom, with no chemical meaning. These data can be obtained free of charge from The Cambridge Crystallographic Data Center via www.ccdc.cam.ac.uk/data_request/cif (CCDC 1882280 **1a** and CCDC 1882281 **1b**) or in the Supplementary Information.

Cell lines

Human renal clear cell carcinoma line Caki-1 and human prostate adenocarcinoma line PC3 were obtained from the American Type Culture Collection (ATCC) (Manassas, Virginia, USA) and cultured using Roswell Park Memorial Institute (RPMI-1640) (Fisher Scientific, Hampton, NH) media containing 10% Fetal Bovine Serum, certified, heat inactivated, US origin (FBS) (Fisher Scientific, Hampton, NH), 1% Minimum Essential Media (MEM) nonessential amino acids (NEAA) (Fisher Scientific, Hampton, NH), and 1% penicillin-streptomycin (PenStrep) (Fisher Scientific, Hampton, NH). Human fetal lung fibroblast IMR90 cells were purchased from ATCC (Manassas, Virginia, USA) and cultured using Dulbecco's modified Eagle's medium (DMEM) (Fisher Scientific, Hampton, NH) supplemented with 10% FBS, 1% MEM-NEAA, and 1% PenStrep. All cells were cultured at 37 °C under 5% CO_2 and 95% air in a humidified incubator.

Cell viability analysis

The cytotoxic profile (IC_{50}) of the compounds were determined by assessing the viability of PC3, Caki-1 and IMR90 cells. Cells were seeded at a concentration of 5 x 103 cells/well in 90 µL of appropriate complete media without phenol red into tissue culture grade 96-well flat bottom microplates (BioLite Microwell Plate, Fisher Scientific, Waltham, MA) and grown for 24 h at 37 °C under 5% CO2 and 95% air in a humidified incubator. The compounds **a**, **1a**, **1b** and **2a** were dissolved in a 1:1 solution of Triethylglycol and DMSO, while compounds **b**, **2b**, **AF** and **Ti-Y** were dissolved in DMSO. Cisplatin was dissolved in H_2O. The intermediate dilutions of the compounds were added to the wells (10 µL) to obtain concentration of 0.1 µM, 1 µM, 10 µM, 50 µM and 100 µM, 0.1% DMSO was used as control, and the cells were incubated for 72 h. Presto Blue was used to quantitively measure variations in cell viability of treated cells. Following 72 h drug exposure, 11 µL per well of 10x PrestoBlue (Invitrogen, Carlsbad, CA) labeling mixture was added to the cells at a final concentration of 1x and incubated for 1 h at 37 °C under 5% CO2 and 95% air in a humidified incubator. The optical fluorescence of each well in a 96-well plate was quantified using a BioTek Synergy Multi-mode microplate reader (BioTek Instruments, Inc., Winooski, VT) set at 530/25 excitation nm and 590/35 nm emission. The percentage of surviving cells was calculated from the ratio of absorbance of treated to untreated cells. The IC_{50} value was calculated as the concentration reducing the proliferation of the cells by 50% and is presented as a mean (±S.EM) of at least two independent experiments each with triplicate measurements.

Cell death assay

For the assessment of the cell death in PC3, cells were cultured in 100 mm tissue culture dishes (Fisher Scientific, Hampton, NH) using RPMI phenol red free medium and reach a growth ~75% confluency. The cells were dose using the IC_{50} of compounds **a**, **1a**, **2a**, **AF** and incubated for 72 h at 37 °C under 5% CO_2 and 95% air in a humidified incubator. Then, cells were collected using trypsin (Fisher Scientific, Hampton, NH) to later count with a hemocytometer and prepare 25 x104 cells/sample. After the samples were prepared, the cells in the samples were centrifuged, supernatant was aspirated from the pallet, and washed gently one time with PBS. The cells were centrifuged again, PBS was aspirated and eBioscience Annexin V-FITC Apop Kit (Invitrogen, Carlsbad, CA) was used to labeled cells as follows, the cells were resuspended in 195 µL of 1x binding buffer and 5 µL of Annexin-V dye was added. The cells were incubated at room temperature for 10 min. After the incubation period finished, cells were washed one time with 1x binding buffer and resuspended in 190 µL of 1x binding buffer with 10 µL of propidium iodide. The dye's fluorescence intensity was detected via

flow cytometry using a BD C6 Accuri flow cytometer. 10 x 105 events per sample were recorded. The flow cytometer was calibrated prior to each use.

Cell migration analysis

PC3 cells were allowed to seed in fibronectin-coated 6-well plate (Corning Incorporated, Durham, NC) and grown a monolayer of ~90% confluency. After which, the monolayer was scratched using a 200 µL tip. The complete medium and cells detached due to the scratch were aspirated and replaced with serum-free medium. The antimigratory profiles of bimetallic compound **2a**, monometallic compounds **a**, **1a**, and **AF** was assessed with the IC_{20} of each compound. The diluting agent (1:1, triethylglycol: DMSO) served as a negative control. Cells were incubated at 37 °C under 5% CO_2 and 95% air in a humidified incubator. At 0, 6, 24 and 48 h after the scratch, cells were photographed using a Leica MC120 HD mounted on a Leica DMi1 microscope at 5x magnification. The area invaded was measured in five randomly selected segments from each photo then averaged. Data were collected from two independent experiments.

Immunohistochemistry

Cells were seeded in an 8-well millicell slide (Millipore, sigma) at a concentration of 25000 cells/well in a humidified atmosphere of 95% air/5% CO2 at 37 °C. 24h post seeding, cells were treated with the IC_{20} of bimetallic compound **2a**, monometallic compound **a**, **1a**, and as control **AF** and incubated for 24 h. Cells were fixed using 4% PFA and incubate at room temperature for 15 min. The PFA was removed and the wells were washed three times with PBS. Cells were handled carefully as to maintain cellular integrity. The cells were then blocked with 5% BSA (Fisher Scientific, Hampton, NH), 0.3% Triton-X100 (Acros Organics, Morris Plains, NJ, USA) in PBS for 1h at room temperature. The blocking solution was then removed and the wells were washed three times with PBS. After the washes with PBS, cells were incubated overnight at 4 °C with the respective antibodies. TrxR activity in cells was visualized using an rabbit anti-thioredoxin antibody (Novus biological, Littleton, CO). VEGF activity was obtained by using mouse anti-VEGF antibody (Novus biological, Littleton, CO) and goat anti-mouse secondary antiody (Fisher Scientific, Hampton, NH). Then, the antibodies solution was removed from the slide and anti-phalloidin antibody (Cell Signaling Technology, Danvers, MA) to visualize the cytoskeleton of the cells. After 1 h of incubation at room temperature, cells were washed three times with PBS and one drop per well of DAPI containing ProLong Gold Antifade Mounting Medium (Invitrogen, Carlsbad, CA) was used to visualize the nuclei and mount the slide.

Analysis of cell TrxR, VEGF, Phalloidin and DAPI.

Following immunohistochemical processing all stained samples were imaged at 10x magnification using Fluoview FV10i (Olympus America Inc., Center Valley, PA). Cell were quantified one channel at a time using ImageJ, and the percentage of rabbit anti-thioredoxin antibody positive per DAPI positive cells were calculate per field of view over 5 fields of view.

Acknowledgements

This work was supported by the National Cancer Institute and the National Institute for General Medical Sciences (NIGMS) grants 1SC1CA182844 and 2SC1 GM127278-05A1 (M.C.). N.C. thanks a postdoctoral fellowship from the Fundación Alfonso Martín Escudero (Spain). N.G thanks the Universidad de La Rioja (Spain) for a doctoral fellowship and a travel scholarship. M.A. thanks the Ministerio de Economía y Ciencia (MINECO) from Spain, for a doctoral fellowship and a travel scholarship. We are extremely grateful to Dr. Benelita T. Elie for advice on some of the biological assays and to Prof. Elena Lalinde (Universidad de la Rioja, Spain) for useful discussions regarding the X-ray crystal structures.

Conflict of Interest

The authors declare no conflict of interest.

Keywords: Heterometallic • titanocene-gold • N-heterocyclic carbenes •prostate cancer • renal cancer

References:

[1] A. Casini, A. Vessières, S.M. Meier-Menches (Eds). In Metal-based Anticancer Agents. Book Series Metallobiology. Royal Society of Chemistry (2019).
[2] J.-X. Liang,H.-J. Zhong, G. Yang, K. Vellaisami, D.-L. Ma, C.-L. Leung. *J. Inorg. Biochem*., **2017**, *177*, 276-286.
[3] C.S. Allardyce, P.J. Dyson. *Dalton Trans*. **2016**, *45*, 3201-3209.
[4] T.C. Johnstone, K. Suntharaligam, S.J. Lippard. *Chem. Rev.*, **2016**, *116*, 3436–3486.
[5] Metallo-Drugs: Development and Action of Anticancer Agents. A. Sigel, H. Sigel, E. Freisinger, R.K.O. Sigel (Eds.), in: Vol. 18 of Metal Ions in Life Sciences. Walter de Gruyter, Berlin, Germany (2018).
[6] B. Engliner, C. Pirker, P. Heffeter, A. Terenzi, C.R. Kowol, B.K. Keppler, W. Berger. *Chem. Rev.* **2019**, *119*, 1519–1624.
[7] S. Monro, K.L. Colón, H. Yin, J. Roque, P. Konda, S. Gujar, R.P. Thummel, L. Lilge, C.G. Cameron, S.A. McFarland. *Chem. Rev.* **2019**, *119*, 797–828.
[8] M. Pourshafiri, M.T. Wlodarczyk, A.J. Mieszawska. *Inorganics*, 2018, 7(1)2.
[9] N. Curado, M. Contel. Heterometallic Compounds as Anticancer Agents (Ch 6). In: Metal-based Anticancer Agents. Book Series Metallobiology. A. Casini, A. Vessières, S.M. Meier-Menches (Eds). Royal Society of Chemistry (2019).
[11] F. Pelletier, V. Comte, A. Massard, M. Wenzel, S. Toulot, P. Richard, M. Picquet, P. Le Gendre, O. Zava, F. Edafe, A. Casini, J.P. Dyson. *J. Med. Chem.* **2010**, *53*, 6923–6933.
[12] J.F. González-Pantoja, M. Stern, A.A. Jarzecki, E. Royo, E. Robles-Escajeda, A. Varela-Ramírez, R.J. Aguilera, M. Contel. *Inorg. Chem.* **2011**, *50*, 11099–11110.
[13] J. Fernández-Gallardo, B.T. Elie, F.J. Sulzmaier, M. Sanaú, J.W. Ramos, M. Contel. *Organometallics*, **2014**, *33*, 6669–6681.
[14] (a) J. Fernández-Gallardo, B.T. Elie, T. Sadhukha, S. Prabha, M. Sanaú, S. Rotenberg, J.W. Ramos, M. Contel. *Chem. Sci.* **2015**, *6*, 5269–5283. (b) M. Contel, J. Fernández-Gallardo, B.T. Elie, J.W. Ramos. US Patent 9,315,531 (04/19/2016).
[15] B.T. Elie, J. Fernández-Gallardo, N. Curado, M.A. Cornejo, J.W. Ramos, M. Contel. *Eur. J. Med. Chem*. **2019**, *161*, 310-322.
[16] Y.F. Mui, J. Fernández-Gallardo, B.T. Elie, A. Gubran, I. Maluenda, M. Sanaú, O. Navarro, M. Contel. Organometallics **2016**, *35*, 1218–1227.
[17] L. Massai, J. Fernández-Gallardo, A. Guerri, A. Arcangeli, S. Pillozzi, M. Contel, L. Messori. *Dalton Trans*. **2015**, *44*, 11067–11076.
[18] J. Fernández-Gallardo, B.T. Elie, M. Sanaú, M. Contel. Chem. Commun. **2016**, *52*, 3155–3158.
[19] B.T. Elie, Y. Pechenyy, F. Uddin, M. Contel. *J. Biol. Inorg. Chem*. **2018**, *23*, 399-411.
[20] F. Hackenberg, H. Muller-Bunz, R. Smith, W. Streciwilk, X. Zhu, M. Tacke. *Organometallics*, **2013**, *32*, 5551-5560.
[21] W. Liu, K. Bensdorf, M. Proetto, U. Abram, A. Hagenbach, R. Gust. *J. Med. Chem*. **2011**, *54*, 8605-8615.

[22] T. Marzo, L. Massai, A. Pratesi, M. Stefanino, D. Cirri, F. Magherini, M. Becatti, I. Landini, S. Nobili, E. Mini, O. Crociani, A. Arcangeli, S. Pillpzzi, T. Gamberi, L. Messori. *ACS Med. Chem. Lett*. **2019**, DOI: 10.1021/acsmedchemlett.9b0000.
[23] B. Bertrand, A. Casini, Dalton Trans. **2014**, *43*, 4209-4219.
[24] T. Zou, C.T. Lum, C.-N. Lok, J.-J. Zhang, C.M. Che. *Chem. Soc. Rev.* **2015**, *44*, 8786-8801.
[25] M. Mora, M.C. Gimeno, R. Visbal. *Chem. Soc. Rev*. **2019** DOI: 10.1039/C8CS00570B.
[26] O. Dada, D. Curran, C. O'Beirne, H. Muller-Bunz, X. Zhu, M. Tacke. *J. Organomet. Chem*. **2017**, *840*, 30-37.
[27] W. Walther, O. Dada, C. O'Beirne, I. Ott, Goar Sánchez-Sanz, C. Schmidt, C. Werner, X. Zhu, M. Tacke. *Lett. Drug Design & Discovery*. **2017**, *14*, 125-134.
[28] M.J. Matos, C. Labao-Almeida, C. Sayers, O. Dada, M. Tacke, G.J.L. Bernardes. *Chem. Eur. J*. **2018**, *24*, 12250-12253.
[29] F. Canales, M.C. Gimeno, A. Laguna, P.G. Jones. *J. Am. Chem. Soc*. **1996,** *118*, 4839-4845.
[30] G.B. Deacon, R.J. Phillips. J. *Coord. Chem. Rev*. **1980**, *33*, 227-250.
[31] D. Martínez, M. Motevalli, M. Watkinson. *Dalton Trans*. **2010**, *39*, 446-455.
[32] B.T. Elie. *Doctoral Dissertation Thesis*. Biology PhD Program, City University of New York, NY, USA, **2018**. https://academicworks.cuny.edu/gc_etds/3060/.
[33] N.J. Sweeney, O. Mendoza, H. Muller-Bunz, C. Pampillon, F.-J.K. Rehmann, K. Strohfeldt, M. Tacke. *J. Organomet. Chem*. **2005**, *690*, 4537-4544**.**
[34] P. Beckhove, O. Oberschmidt, A.R. Hanauske, C. Pampillón, V. Schirrmacher, N.J. Sweeney, K. Strohfeldt, M. Tacke. *Anti-Cancer Drugs*. **2007**,*18*, 311-315.
[35] J.H. Bannon, I. Fitchner, A. O'Neill, C. Pampillón, N.J. Sweeney, K. Strohfeldt, R.W. Watson, M. Tacke, M.M. Mc Gee. *Br. J. Cancer*, **2007**, *97*, 1234-1241.
[36] I. Fichtner, C. Pampillón, N.J. Sweeney, K. Strohfeldt, M. Tacke. *Anti-Cancer Drugs*. **2006**, *17*, 333-336.
[37] C. Roder, M. Thomson. *Drugs in R&D*, **2015**, *15*, 13–20 and refs. therein.
[38] A. Nakaya, M. Sagawa, A. Muto, H. Uchida, Y. Ikeda, M. Kizaki. *Leukemia Res.* **2011**, *35*, 243–249.
[39] K. O'Connor, C. Gill, M. Tacke, F.-J.K. Rehmann, K. Strohfeldt, N. Sweeney, J.M. Fitzpatrick, R.W.G. Watson. Apoptosis, **2016**, 11, 1205–1214.
[40] M.R. Ray, D.M. Jablons. Hallmarks of Metastasis. In: Lung Cancer Metastasis (Eds: V. Keshamouni, D. Arenberg, G. Kalemkerian) Springer, New York, NY, **2009**.
[41] W. Zhang, K. Kai, N.T. Ueno, L. Quin. *Cancer Hallm*. **2013**, 1, 59-66.
[42] S. Lee, S.M. Kim, R.T. Lee. *Antioxidants & redox signaling*. **2013**, *18*, 1165-207.
[43] K.L. Streicher, M.J. Sylte, S.E. Johnson, L.M. Sordillo. *Nutr. Cancer*. **2014**, 50, 221-231.
[44] C. Chen, L. Li, H.J. Zhou, W. Min. *Antioxidants*, **2017**, 6, pii:E42.
[45] T.C. Karlenius, K.F. Tonissen. *Cancers*, **2010**, *2*, 209–232.
[46] P. Wang, Y. Wu, X. Li, X. Ma, L. Zhong. *J. Biol. Chem*. **2013**, *288*, 3346-3358.
[47] R. Roskoski Jr. *Crit. Rev. Oncol. Hematol*. **2007**, *62*, 179-213.
[48] O. López-Ocejo, A. Viloria-Petit, M. Bequet-Romero, D. Mukhopadhyay, J. Rak, R.S. Kerbel. *Oncogene*, **2000**, *19*, 4611-4620.
[49] J. Rak, Y. Mitsuhashi, C. Sheehan, A. Tamir, A. Viloria-Petit, J. Filmus, S.J. Mansour, N.G. Ahn, R.S. Kerbel. *Cancer Res*. **2000**, *60*, 490-498.
[50] C.E. Gilet. *Humana Press*, **2016**, 120.
[51] R. Blanco. *Immunol. Curr. Res*. **2017**, *1* (1).
[52] R. Usón, A. Laguna, M. Laguna. *Inorg. Synth*. **1989**, *26*, 85-91.
[53] J.F. Payack, D.L. Hughes, D. Cai, I.F. Cottrell, T.R. Verhoeven. *Org. Synth*. **2002**, *79*, 19.
[54] Gaussian 09, Revision C.01, M. J. Frisch, G. W. Trucks, H. B. Schlegel, G. E. Scuseria,M. A. Robb, J. R. Cheeseman, G. Scalmani, V. Barone, B. Mennucci, G. A. Petersson, H. Nakatsuji, M. Caricato, X. Li, H. P., Hratchian, A. F. Izmaylov, J. Bloino, G. Zheng, J. L. Sonnenberg, M. Hada, M. Ehara, K. Toyota, R. Fukuda, J. Hasegawa, M. Ishida, T., Nakajima, Y. Honda, O. Kitao, H. Nakai, T. Vreven, J. A. Montgomery, Jr., J. E. Peralta, F. Ogliaro, M. Bearpark, J. J. Heyd, E. Brothers, K. N. Kudin, V. N. Staroverov, T. Keith, R. Kobayashi, J. Normand, K. Raghavachari, A. Rendell, J. C. Burant, S. S. Iyengar, J. Tomasi, M. Cossi, N. Rega, J. M. Millam, M. Klene, J. E. Knox, J. B. Cross, V. Bakken, C. Adamo, J. Jaramillo, R. Gomperts, R. E. Stratmann, O. Yazyev, A. J. Austin, R. Cammi, C. Pomelli, J. W. Ochterski, R. L. Martin, K. Morokuma, V. G. Zakrzewski, G. A. Voth, P. Salvador, J. J. Dannenberg, S. Dapprich, A. D. Daniels, O. Farkas, J. B. Foresman, J. V. Ortiz, J. Cioslowski, D. J. Fox, Gaussian, Inc., Wallingford CT, 2010.
[55] A. Canal Neto, F. E. Jorge. *Chem. Phys. Lett*. **2013**, *582*, 158-162.
[56] K.L. Schuchardt, B.T. Didier, T. Elsethagen, L. Sun, V. Gurumoorthi, J. Chase, J. Li, T.L. Windus. *J. Chem. Inf. Model*., **2007**, *47*, 1045-1052.
[57] G.M. Sheldrick. SHELXT – Integrated space-group and crystal structure determination. Acta Crystallogr., Sect. A, **2015**, *71*, 3-8.
[58] G.M. Sheldrick. Crystal structure refinement with SHELXL. *Acta Crystallogr., Sect. C*. **2015**, *71*, 3-8.
[59] R.H. Blessing. An empirical correction for absorption anisotropy. *Acta Crystallogr*. **1995**, *A51*, 33-38.
[60] L.J. Farrugia. WinGX suite for small-molecule single-crystal crystallography. *Appl. Crystallogr*. **1999**, *32*, 837-838.

Entry for the Table of Contents

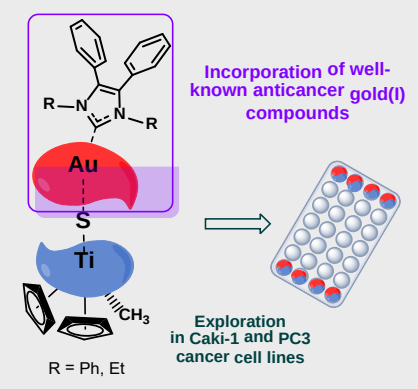

Anticancer Bimetallics*

*Natalia Curado, Nora Giménez, Kirill Miachin, Mélanie Aliaga-Lavrijsen, Mike A. Cornejo, A.A. Jarzecki and María Contel**

Incorporation of a titanocene motif to previously described gold(I) compounds containing *N*-heterocyclic carbene ligands improves or does not decrease their cytotoxicity in human renal and prostate PC3 cancer cell lines. Bimetallic compounds display an improved pharmacological profile in terms of apoptosis, inhibition of migration and inhibition of thioredoxin reductase (TrRx) and vascular endothelial growth factor (VEGF) in prostate cancer cell lines.